Supporting Information

Synthesis of a Cu-filled $Rh_{17}S_{15}$ Framework: Microwave Polyol Process *versus* High-Temperature Route

Maria Roslova[*†], *Pavlo Golub*[†], *Lars Opherden*[‡§], *Alexander Ovchinnikov*[‖], *Marc Uhlarz*[‡], *Alexey I. Baranov*[†‖], *Yurii Prots*[‖], *Anna Isaeva*[†], *Mauro Coduri*[⊥], *Thomas Herrmannsdörfer*[‡], *Joachim Wosnitza*[‡§], *Thomas Doert*[†] *and Michael Ruck*[†‖]

[†]Department of Chemistry and Food Chemistry, Technische Universität Dresden, 01062 Dresden, Germany

[‖]Max Planck Institute for Chemical Physics of Solids, 01187 Dresden, Germany

[‡]Dresden High Magnetic Field Laboratory (HLD-EMFL), Helmholtz-Zentrum Dresden-Rossendorf, 01314 Dresden, Germany

[§]Institute for Solid State Physics, Technische Universität Dresden, 01062 Dresden, Germany

[⊥]ESRF – The European Synchrotron, 38043 Grenoble, France

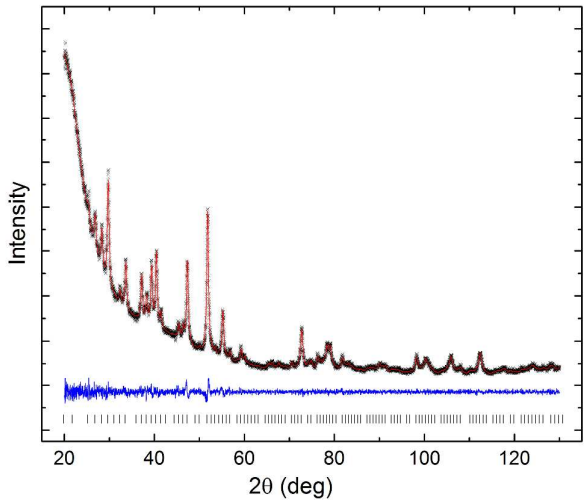

Figure S1. The Rietveld fit of the XRD pattern for the as-prepared sample obtained by microwave-assisted synthesis (Sample 1) (experimental data denoted as black crosses), including the profile fit (red solid line) and profile difference (blue solid line). The peak positions of $Cu_3Rh_{34}S_{30}$ are indicated by black ticks. The XRD pattern registered with the Cu$K_{\alpha 1}$ radiation.

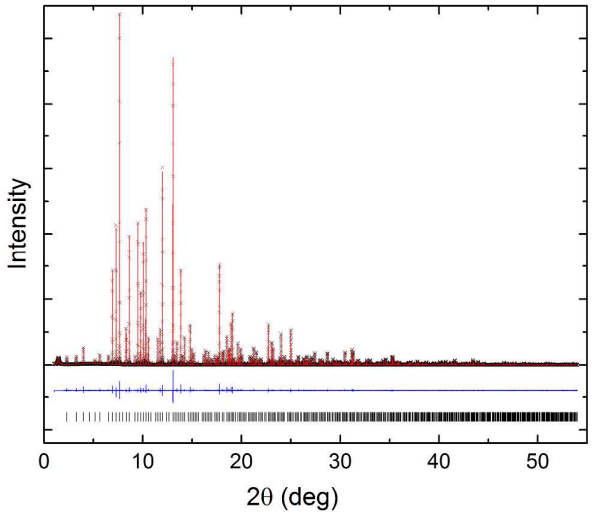

Figure S2. The Rietveld fit of the XRD pattern for the $Cu_{3-\delta}Rh_{34}S_{30}$ sample (Sample 3) obtained by high-temperature reaction (experimental data denoted as black crosses), including the profile fit (red solid line) and profile difference (blue solid line). The refined peak positions are indicated by black ticks. The XRD pattern registered with the synchrotron radiation (λ = 0.40001 Å). The region between 1.002 ° and 1.966 ° was excluded from the

refinement since the signal is caused by the kapton window of the cryostat at low angles and no diffraction peaks were expected in this region.

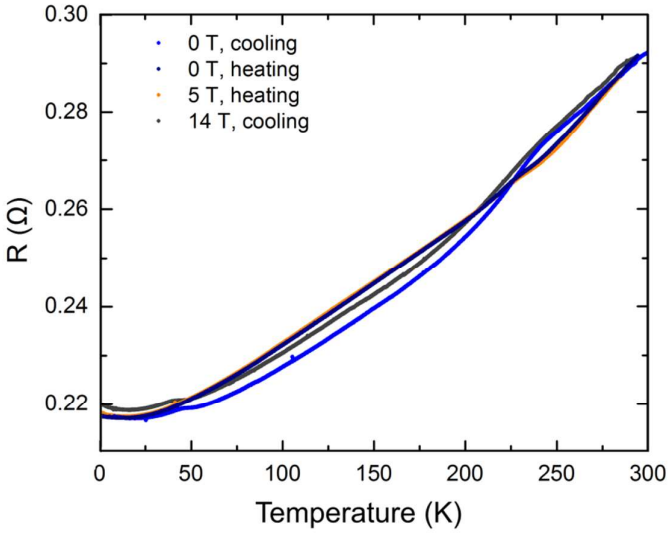

Figure S3. Resistivity versus temperature at different applied fields (H = 0, 5, 14 T). Between 40 K and 225 K the measured resistivity shows thermal hysteresis for all applied field values.

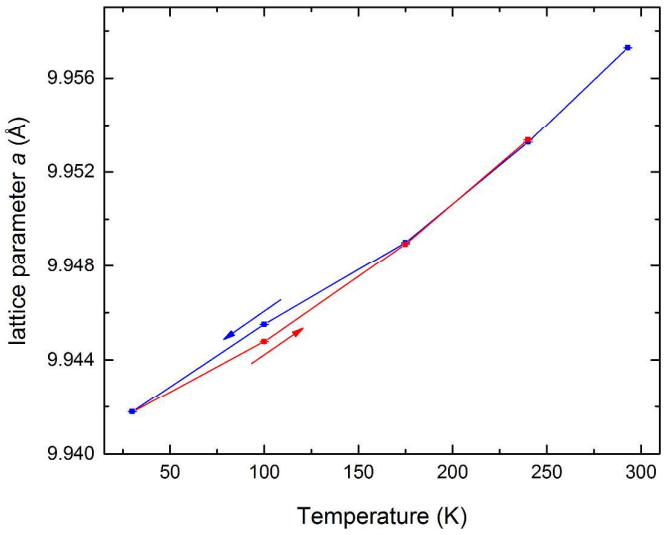

Figure S4. Temperature evolution of the lattice parameter for Sample 3. Blue arrow indicates the cooling cycle, red arrow – the heating cycle.

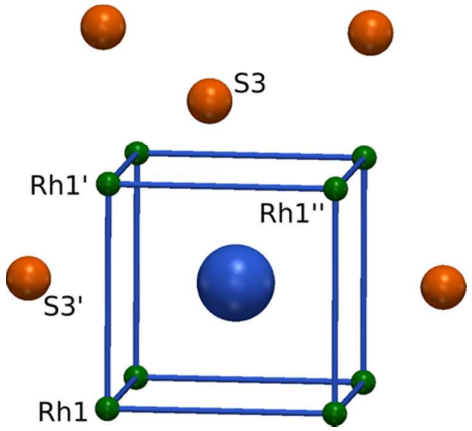

Figure S5. The atom labels used in Table S3.

Table S1. Atomic Coordinates and Displacement Parameters for the $Cu_{3-\delta}Rh_{34}S_{30}$ samples (space group $Pm\bar{3}m$, $Z = 1$).

Atom	Site	x	y	z	U_{iso} (Å^2)
Sample 1 (δ = 0)					
Rh1	24*m*	0.3527(1)	x	0.1483(2)	0.0134(4)
Rh2	6*e*	0.2377(3)	0	0	0.0134
Rh3	3*d*	½	0	0	0.0134
Rh4	1*b*	½	½	½	0.0134
S1	12*j*	½	0.1676(6)	y	0.0157(13)
S2	12*i*	0	0.2287(5)	y	0.0157
S3	6*f*	0.2639(11)	½	½	0.0157
Cu1	3*c*	0	½	½	0.0134
Sample 2 (δ = 2.10(2))					
Rh1	24*m*	0.3551(1)	x	0.1448(2)	0.0171(5)
Rh2	6*e*	0.2388(3)	0	0	0.0171
Rh3	3*d*	½	0	0	0.0171
Rh4	1*b*	½	½	½	0.0171
S1	12*j*	½	0.1685(4)	y	0.0156(9)
S2	12*i*	0	0.2300(5)	y	0.0156
S3	6*f*	0.2671(10)	½	½	0.0156
Cu1	3*c*	0	½	½	0.0171
Sample 3 (δ = 1.32(2))					
Rh1	24*m*	0.35413(6)	x	0.1448(2)	0.0155(2)
Rh2	6*e*	0.2389(2)	0	0	0.0155
Rh3	3*d*	½	0	0	0.0155
Rh4	1*b*	½	½	½	0.0155
S1	12*j*	½	0.1685(2)	y	0.0131(5)
S2	12*i*	0	0.2295(2)	y	0.0131
S3	6*f*	0.2676(5)	½	½	0.0131
Cu1	3*c*	0	½	½	0.0155

Sample 4 (δ = 0.94(2))					
Rh1	24*m*	0.3536(6)	x	0.1475(10)	0.0100(2)
Rh2	6*e*	0.236(2)	0	0	0.0100
Rh3	3*d*	½	0	0	0.0100
Rh4	1*b*	½	½	½	0.0100
S1	12*j*	½	0.168(3)	y	0.014(7)
S2	12*i*	0	0.225(3)	y	0.014
S3	6*f*	0.265(3)	½	½	0.014
Cu1	3*c*	0	½	½	0.0100
Sample 5 (δ = 0.96(2))					
Rh1	24*m*	0.35341(17)	x	0.1467(2)	0.0175(6)
Rh2	6*e*	0.2385(5)	0	0	0.0175
Rh3	3*d*	½	0	0	0.0175
Rh4	1*b*	½	½	½	0.0175
S1	12*j*	½	0.1701(7)	y	0.0205(16)
S2	12*i*	0	0.2292(8)	y	0.0205
S3	6*f*	0.269(2)	½	½	0.0205
Cu1	3*c*	0	½	½	0.0175
Sample 6 (δ = 1.94(2))					
Rh1	24*m*	0.3546(5)	x	0.1456(7)	0.0114(14)
Rh2	6*e*	0.237(1)	0	0	0.0114
Rh3	3*d*	½	0	0	0.0114
Rh4	1*b*	½	½	½	0.0114
S1	12*j*	½	0.169(2)	y	0.015(5)
S2	12*i*	0	0.231(2)	y	0.015
S3	6*f*	0.261(5)	½	½	0.015
Cu1	3*c*	0	½	½	0.0114

Comment: U_{iso} for all the Rh atoms as well as U_{iso} for all the S atoms are constrained.

$U_{iso}(Cu1) = U_{iso}(Rh^{*})$ constrained.

Table S2. Selected Bond Lengths (Å) and Angles (deg) for the $Cu_{3-\delta}Rh_{34}S_{30}$ samples.

Atoms	Bond Length, Å	Atoms	Angle, deg
Sample 1 (δ = 0)			
Rh1—S2	2.298(5)	S1—Rh1—S1	164.0(2)
Rh1—S1	2.365(5)	S1—Rh1—S2	88.3(2)
Rh1—S3	2.381(7)	S1—Rh1—S3	93.2(1)
Rh1—Cu1	2.5554(16)	S2—Rh1—S3	168.9(3)
Rh2—S2	2.282(6)	S2—Rh2—S2	174.8(3)
Rh2—Rh3	2.611(4)		
Rh3—S1	2.378(7)		
Rh4—S3	2.358(9)		
Sample 2 (δ = 2.10(2))			
Rh1—S2	2.273(2)	S1—Rh1—S1	161.76(7)
Rh1—S1	2.359(2)	S1—Rh1—S2	88.09(8)
Rh1—S3	2.369(3)	S1—Rh1—S3	93.22(5)
Rh1—Cu1	2.4952(7)	S2—Rh1—S3	171.36(12)

Rh2—S2	2.286(3)	S2—Rh2—S2	175.53(12)
Rh2—Rh3	2.595(2)		
Rh3—S1	2.367(2)		
Rh4—S3	2.319(5)		
Sample 3 (δ = 1.32(2))			
Rh1—S2	2.276(6)	S1—Rh1—S1	162.5(2)
Rh1—S1	2.358(5)	S1—Rh1—S2	88.4(2)
Rh1—S3	2.276(6)	S1—Rh1—S3	93.0(1)
Rh1—Cu1	2.5150(10)	S2—Rh1—S3	170.7(3)
Rh2—S2	2.288(7)	S2—Rh2—S2	175.4(3)
Rh2—Rh3	2.276(6)		
Rh3—S1	2.377(6)		
Rh4—S3	2.322(4)		
Sample 4 (δ = 0.94(2))			
Rh1—S2	2.271(4)	S1—Rh1—S1	163.3(1)
Rh1—S1	2.357(3)	S1—Rh1—S2	88.6(2)
Rh1—S3	2.397(5)	S1—Rh1—S3	92.74(9)
Rh1—Cu1	2.535(1)	S2—Rh1—S3	170.1(2)
Rh2—S2	2.291(5)	S2—Rh2—S2	175.5(2)
Rh2—Rh3	2.604(3)		
Rh3—S1	2.383(4)		
Rh4—S3	2.316(9)		
Sample 5 (δ = 0.96(2))			
Rh1—S2	2.281(7)	S1—Rh1—S1	163.0(2)
Rh1—S1	2.351(6)	S1—Rh1—S2	88.8(3)
Rh1—S3	2.397(9)	S1—Rh1—S3	92.6(2)
Rh1—Cu1	2.531(2)	S2—Rh1—S3	170.6(4)
Rh2—S2	2.286(8)	S2—Rh2—S2	175.4(4)
Rh2—Rh3	2.607(5)		
Rh3—S1	2.397(7)		
Rh4—S3	2.305(9)		
Sample 6 (δ = 1.94(2))			
Rh1—S2	2.351(6)	S1—Rh1—S1	163.0(2)
Rh1—S1	2.351(6)	S1—Rh1—S2	88.8(3)
Rh1—S3	2.397(9)	S1—Rh1—S3	92.6(2)
Rh1—Cu1	2.531(2)	S2—Rh1—S3	170.6(4)
Rh2—S2	2.286(8)	S2—Rh2—S2	175.4(4)
Rh2—Rh3	2.607(5)		
Rh3—S1	2.397(7)		
Rh4—S3	2.305(9)		

Table S3. The states treated as valence in the electronic structure calculations.

Method	Cu	Rh	S
FPLO	3*s*, 3*p*, 3*d*, 4*s*, 4*p*, 4*d*, 5*s*	4*s*, 4*p*, 4*d*, 5*s*, 5*p*, 5*d*, 6*s*	2*s*, 2*p*, 3*s*, 3*p*, 3*d*, 4*s*, 4*p*
PAW	3*s*, 3*p*, 3*d*, 4*s*	4*s*, 4*p*, 4*d*, 5*s*	3*s*, 3*p*

Table S4. The QTAIM basin populations (Q) and the delocalization indices (δ) for $Rh_{17}S_{15}$ and $Cu_3Rh_{34}S_{30}$. (atoms labeled according to Figure S5).

	$Rh_{17}S_{15}$	$Cu_3Rh_{34}S_{30}$
Q(Rh)	44.71	44.66
Q(S)	16.33	16.41
Q(Cu)	-	28.77
δ(Rh1'-Rh1")	0.35	0.26
δ(Rh1-Rh1')	0.25	0.20
δ(Rh1'-S3)	0.79	0.70
δ(Rh1-S3')	0.69	0.65
δ(Rh1'-Cu)	-	0.35
δ(Cu-S3')	-	0.15

Table S5. The occupation numbers and the degree of localization (percentage of the orbital norm representing orbital charge) for DAFH orbitals of Cu QTAIM atom in fcc-Cu and $Cu_3Rh_{34}S_{30}$.

Compound	DAFH orbitals	occ. number	orbital norm inside the reference basin
fcc-Cu	*s*-type	0.69	36%
	p-type	0.24	14%
	d-type	1.86-1.89	94-96%
$Cu_3Rh_{34}S_{30}$	*s*-type	0.62	31%
	p-type	0.18-0.22	9-11%
	d-type	1.79-1.93	93-97%